

# Quantum-optical spectroscopy of a two-level system using an electrically driven micropillar laser as resonant excitation source

Sören Kreinberg,<sup>1</sup> Tomislav Grbešić,<sup>1</sup> Max Strauß,<sup>1</sup> Alexander Carmele,<sup>2</sup> Monika Emmerling,<sup>3</sup> Christian Schneider,<sup>3</sup> Sven Höfling,<sup>3,4</sup> Xavier Porte,<sup>1</sup> and Stephan Reitzenstein<sup>1,\*</sup>

<sup>1</sup>*Institut für Festkörperphysik, Technische Universität Berlin, Germany*

<sup>2</sup>*Institut für Theoretische Physik, Technische Universität Berlin, Germany*

<sup>3</sup>*Technische Physik, Julius-Maximilians-Universität Würzburg, Germany*

<sup>4</sup>*SUPA, School of Physics and Astronomy, University of St Andrews, St Andrews, KY16 9SS, United Kingdom*

Two-level emitters constitute main building blocks of photonic quantum systems and are model systems for the exploration of quantum optics in the solid state. Most interesting is the strict-resonant excitation of such emitters to generate close to ideal quantum light and to control their occupation coherently. Up till now related experiments have been performed exclusively using bulky lasers which hinders the application of resonantly driven two-level emitters in photonic quantum systems. Here we perform quantum-optical spectroscopy of a two-level system using a compact high- $\beta$  microlaser as excitation source. The two-level system is based on a semiconductor quantum dot (QD), which is excited resonantly by a fiber-coupled electrically driven micropillar laser. In this way we dress the excitonic state of the QD under continuous wave excitation and trigger the emission of single-photons with strong multi-photon suppression ( $g^{(2)}(0) = 0.02$ ) and high photon indistinguishability ( $V = 57 \pm 9\%$ ) via pulsed resonant excitation at 156 MHz.

The physics of two-level systems constitutes the basis for quantum optics and quantum cavity electrodynamics (cQED). It has also important impact in the field of photonic quantum technologies where it enables the secure exchange of information via single photons.<sup>1-4</sup> In this context, semiconductor quantum dots (QDs) are close to ideal two-level systems and can act as triggered sources of single photons.<sup>5</sup> In order to explore their physics and the quantum nature of emission, different excitation schemes have been developed which include simple non-resonant electrical and optical excitation as well as more advanced schemes like wetting-layer or p-shell resonant excitation.<sup>6-11</sup> Most interesting is strict-resonant excitation of the fundamental QD transition leading to resonance fluorescence.<sup>12-14</sup> From an experimental point of view, strict-resonant excitation is very demanding because it requires laser stray-light suppression by typically more than 6 orders of magnitude.<sup>15-17</sup> Nevertheless, the development of efficient suppression schemes and the availability of mode-hop-free tunable lasers has led to huge progress in this field and resonance fluorescence has become an important experimental technique in quantum nanophotonics. Strict-resonant excitation has for instance been used to study the subnatural linewidth from a single quantum dot<sup>18</sup> and to explore the non-resonant dot-cavity coupling in microcavity systems.<sup>19</sup> It is interesting to note that up until now related experiments have exclusively been performed using bulky and expensive tunable lasers.

In view of applications in quantum communication, strict-resonant excitation of QDs is very advantageous because it leads to the emission single photons with close to ideal quantum properties in terms of multiphoton suppression and photon indistinguishability.<sup>14</sup> Both aspects are crucial for advanced quantum communication protocols based on entanglement distribution via Bell-state

measurements.<sup>20,21</sup> In addition, to enable "real-world" applications it is highly interesting to develop compact electrically driven quantum light sources. Unfortunately, standard excitation schemes based on carrier injection via a pin-diode design are intrinsically non-resonant which limits the achievable degree of indistinguishability.<sup>22</sup> To overcome this issue an advanced excitation concept has been developed using an electrically driven microlaser to excite a single quantum dot in a nearby microcavity system.<sup>23</sup> In this concept, quasi-resonant p-shell excitation was shown<sup>24</sup> but strict-resonant excitation has not yet been achieved. In a similar scheme a light emitting diode was used for on-chip excitation of a single quantum dot.<sup>25</sup>

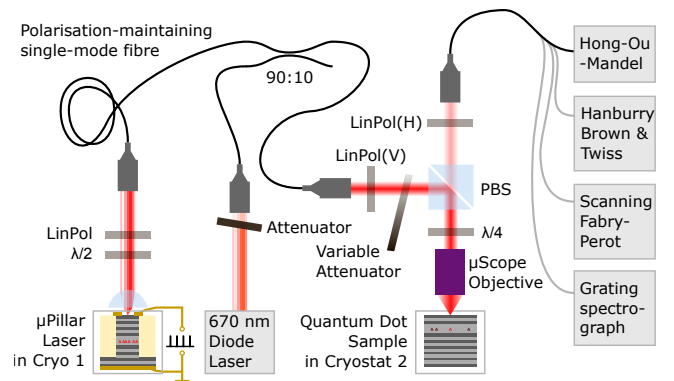


Figure 1. Schematic illustration of the experimental concept: Emission of the electrically driven microlaser in cryostat 1 is fiber-coupled to resonantly excite a single QD in cryostat 2. Applying either CW or pulsed excitation, dressing of the two-level system or triggered emission of single photons can be observed and verified by means of high-resolution spectroscopy and single-photon counting.

In this letter we demonstrate a fully nanophotonic approach to resonantly drive a QD acting as two-level system and to generate single photons with excellent multiphoton suppression and a high degree of photon indistinguishability. Our concept is based on an electrically driven quantum dot micropillar laser which resonantly drives a single QD located in a planar microcavity. In order to resonantly excite a two-level system we use a microlaser spectrally matched to a quantum dot, where the temperature of the microlaser is used as fine-tuning knob in resonance scans. The experiments are performed under continuous wave (CW) and pulsed excitation of the electrically driven microlaser to observe Mollow-triplet spectra and the triggered emission of single photons with a Hong-Ou-Visibility of 60%, respectively. Our results show the potential of high- $\beta$  microlasers (in this case  $\beta = 1\%$ , see SI) to act as excitation sources in quantum optics experiments and constitute an important step towards integrated quantum nanophotonic circuits which rely on a small scale coherent light source for resonant excitation of quantum emitters.

Our experimental concept is illustrated in Fig. 1. It includes a QD-micropillar laser which is located in cryostat 1 and a spectrally matched QD in cryostat 2. The light emitted by the microlaser is coupled into a 10 m long polarization-maintaining single-mode fiber which is connected to the input port of the resonance fluorescence setup to excite the selected QD in cryostat 2. The microlaser is driven by an electrical voltage supply capable of delivering an adjustable DC bias and voltage pulses with a minimum width of 520 ps and an amplitude of up to 8 volt at a repetition rate of up to 312.5 MHz. Resonance tuning with a tuning range of about 35 GHz is enabled by changing the temperature of the microlaser in the range of 64 K to 68 K. The sample temperature of cryostat 2 is set to 7 K to minimize phonon induced decoherence<sup>26</sup> and carrier escape from the QDs in resonance fluorescence experiments. See Methods section for details on the sample technology and on the experimental setup.

For the planned quantum-optical studies it is crucial to couple emission of the high- $\beta$  microlaser with sub-microwatt output power very efficiently into a single-mode fiber connecting the two cryostats. For this purpose we collimate the microlaser emission via a single low-loss  $f = 20$  mm aspheric lens in front of the optical window of cryostat 1. In this context, we would like to note that a slight deviation of the circular cross-section splits the fundamental transverse micropillar mode into two gain-coupled mode components with a spectral splitting of 11 GHz. One of the two modes wins the gain competition and undergoes the lasing transition.<sup>27,28</sup> Emission of the lasing mode is selectively coupled to the polarization-maintaining single-mode fiber via suitable orientation of a half-wave plate placed in the collimated beam path and a subsequent beam-coupler.

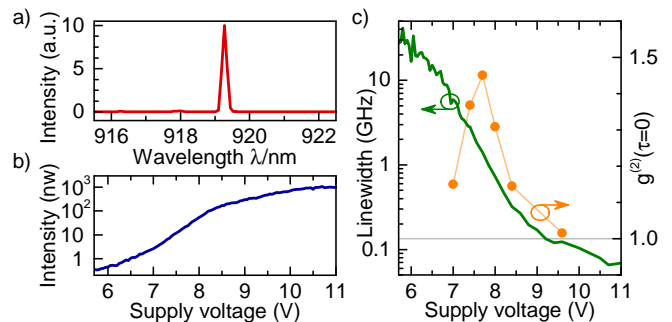


Figure 2. Characterization of the electrically driven micropillar laser under CW excitation: **a)**  $\mu$ EL-spectrum of the QD-micropillar laser showing clean emission of the fundamental mode. Higher-order lateral modes of the micropillar are well suppressed (see SI for details). **b)** Input-Output dependence of the electrically driven QD-micropillar laser with a threshold pump voltage of about 7 - 8 V. **c)** Equal-time second-order photon autocorrelation function (as measured) and spectral linewidth of the QD-microlaser (deconvoluted). The non-linear input-output characteristics in conjunction with the narrowing of emission linewidth by more than three orders of magnitude and the transition of  $g^{(2)}(0)$  from values larger than one to unity are clear indications of predominantly stimulated emission of the QD-microlaser above threshold.

## RESULTS

In the following we apply an electrically driven microlaser to demonstrate for the first time the high potential of micro- and nanolasers in quantum-optical spectroscopy. Indeed, while the research interest on miniaturized lasers has increased rapidly in recent years, their applicability as resonant excitation sources in quantum nanophotonics has been widely unexplored up until now. To enable related studies under strict-resonant excitation, it is crucial to find a microlaser which a) can be operated electrically under CW and pulsed operation with an emission pulse-width significantly shorter than the spontaneous emission lifetime (here 510 ps) of the QD, b) shows single-mode emission with an emission linewidth significantly smaller than the homogeneous linewidth of about 1 GHz, c) is spectrally matched with a target QD within the available temperature-tuning range in the order of 500 GHz, and d) has sufficiently high optical output power of about 100 - 500 nW at the single-mode fiber output to at least saturate the QD transition.

To meet these stringent requirements we first performed reference measurements using a conventional tunable laser as excitation source to select a QD showing pronounced and clean resonance fluorescence at 920 nm (see SI for more detail on the reference measurement), where 920 nm corresponds to the central wavelength reachable by the micropillar lasers within the patterned array. In the second step we chose a micropillar laser with slightly shorter emission wavelength of 919 nm at 10 K, so that it can be spectrally matched with the QD wavelength

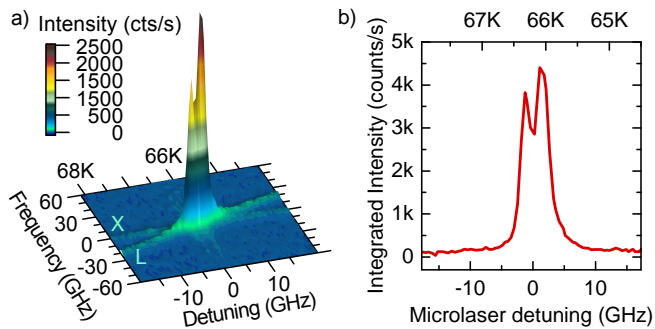


Figure 3. Resonance fluorescence (RF) of a single QD under CW microlaser-excitation ( $V_{\text{bias}} = 10.2 \text{ V}$ ): **a**) 3D surface plot of the QD emission intensity as a function of the frequency  $f$  and the microlaser detuning  $\Delta$ . Using temperature-tuning in a range of 64 - 68 K the laser emission (L) is tuned through the spectral resonance of the selected QD transition (X). Strong RF signal is observed in resonance at about 66 K. **b**) Emission intensity of the QD vs. laser detuning integrated over the spectral range displayed in **a**  $-60 \text{ GHz} \leq f \leq 60 \text{ GHz}$ . The double peak structure is attributed to the fine-structure splitting of the excitonic transition.

at 66 K. Fig. 2a shows the 32 K  $\mu\text{EL}$  emission spectrum of the microlaser at the output of the single-mode fiber. Without any spectral filtering we observe clear single-mode emission with a side mode suppression ratio of 19 dB and no significant contribution from GaAs or wetting layer emission (see SI). Emission of the laser is coupled into a single-mode fiber and leads to an output power of 350 nW at  $V_{\text{bias}} = 10.2 \text{ V}$  at the fiber-output.

Figs. 2b and c present the corresponding voltage-dependent output power and spectral linewidth of the micropillar laser, respectively. The onset of laser action is indicated by the non-linear increase of the output intensity between  $V_{\text{bias}} = 7\text{-}8 \text{ V}$  accompanied with a strong decrease of the emission linewidth to values well below 0.1 GHz. The associated transition from predominantly spontaneous emission to stimulated emission is confirmed by measurements of the bias voltage dependent second-order photon-autocorrelation function  $g^{(2)}(\tau)$ , which shows the typical bunching behavior in the threshold region with  $g^{(2)}(0) > 1$  and a transition towards coherent emission associated with  $g^{(2)}(0) = 1$  at high excitation.<sup>29,30</sup> It is worth noting that the equal-time photon-correlation only approaches  $g^{(2)}(0) = 1$ , when the linewidth is already reduced by a factor of 100 in accordance with Ref.<sup>31</sup>

## DISCUSSION

Having fulfilled all requirements a)-d) discussed above we are prepared for resonance fluorescence (RF) experiments using the selected QD-micropillar laser as coherent excitation source. For this purpose the temperature of the fiber-coupled microlaser in cryostat 1 is gradually

varied between 64 K and 68 K and emission of the QD in the cryostat 2 is recorded via the attached RF setup. The corresponding emission spectra (under CW excitation) are presented Fig. 3a as color-scale intensity map. While under resonant conditions for QD-laser detuning larger than 10 GHz only weak emission of the QD and strongly suppressed laser emission can be detected, strong and very pronounced RF emission occurs at resonance. In fact, when scanning the microlaser emission over the QD s-shell resonance, a double-peaked response with a splitting of 5 GHz detuning can be resolved, see Fig. 3b. This splitting is attributed to the fine-structure splitting of the excitonic transition of the quantum dot.<sup>32</sup> The measurements presented in Figs. 3a and b also point out, that the contribution of reflected laser light and the contribution of QD emission due to above-band excitation by the red laser contributes marginally to the RF signal.

Coherent excitation of the QD based two-level system is demonstrated in Fig. 4. Changing the bias voltage of the micropillar laser we cover a CW excitation power range of 35 nW to 400 nW. Fig. 4a shows the corresponding emission spectra recorded with a high-resolution Fabry-Perot scanning interferometer. With increasing excitation power we observe the characteristic line-broadening of the single emission line with a measured FWHM of 600 MHz at low drive towards the evolution of the Mollow-triplet at high excitation strength.<sup>33</sup> The splitting of the outer lines of the Mollow-triplet with respect to the center amounts to 640 MHz at 350 nW. The occurrence of this important signature of coherent excitation is confirmed for the studied QD by reference measurements over a wider range of excitation powers using a standard tunable laser (see SI).

The quantum nature of RF emission is investigated by measuring the second-order photon auto-correlation function  $g^{(2)}(\tau)$ , again under CW excitation via the electrically driven microlaser. As can be seen Fig. 4b the excitation power dependent photon-correlation reveals pronounced anti-bunching statistics with strong suppression of multi-photon emission events associated with  $g^{(2)}(0) < 0.4$ . Upon increasing the excitation power from 40 nW to 400 nW the simple antibunching dip evolves into a periodically modulated auto-correlation function. The observed signatures are associated with Rabi-oscillations in agreement with the Mollow-triplet observed in frequency domain in Fig. 4a. Noteworthy, we observe  $g^{(2)}(\tau) > 1$  in the vicinity of zero time delay  $\tau \approx 0$ . This photon-bunching increases slightly with excitation power and indicates blinking of the QD due to metastable processes.<sup>34</sup>

In order to obtain more detailed insight into the RF emission features and to theoretically describe the experimental data presented in Fig. 4 we consider the QD as two level system with a spontaneous emission lifetime  $T_1$ , a dephasing time  $T_2$ , and an excitation power-dependent Rabi frequency  $\Omega$ . The properties  $T_1 = 510 \text{ ps}$  and  $\Omega/\sqrt{P} = 2\pi \times 1.33 \text{ THz W}^{-1/2}$  were determined via time resolved experiments under pulsed micropillar laser excitation (cf. Fig. 5) and via excitation power dependent

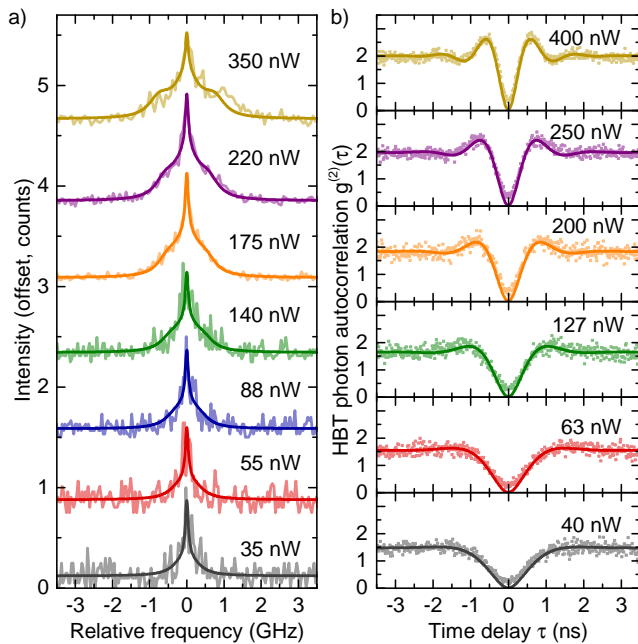


Figure 4. Excitation dependent resonance fluorescence (RF) emission spectra and photon-autocorrelation function under CW microlaser-excitation: **a)** High resolution RF emission spectra for different excitation powers. With increasing excitation power we observe a transition of a single emission line towards a Mollow-triplet like emission spectrum. **b)** Second-order photon auto-correlation function  $g^{(2)}(\tau)$  of the resonantly driven QD. The strong anti-bunching at zero time delay  $\tau = 0$  indicates single-photon emission. At higher laser powers, the narrowing of the anti-bunching peak together with the directly visible Rabi oscillations indicate coherent excitation of the two-level system.

auto-correlation investigations using a standard tunable laser (see SI), respectively.

Using the formulas introduced in the SI we are able to model the experimental data under variation of  $T_2$ . All optimum values of  $T_2$  lie in the vicinity of 500 ps. Assuming  $T_2 = 500$  ps as given, we obtain excellent quantitative agreement between experiment and theory as can be seen in Fig. 4a and Fig. 4b, where solid lines present the calculated data from formulas S3 and S4, respectively.

With respect to applications in photonic quantum technology it is crucial to demonstrate the triggered emission of single photons with excellent quantum properties. For this purpose we biased the microlaser with  $V_{\text{bias}} = 4.71$  V below the onset of lasing and superimposed voltage pulses with  $V_{\text{pp}} = 8$  V with width of 520 ps and a repetition period of 6.4 ns. It is interesting to note that due to the nonlinear input-output dependence of the microlaser the resulting optical emission pulses were shortened significantly to a width of 200 ps (FWHM). The ratio of the peak laser intensity to the strongest afterpulsing intensity was larger than 18 dB (see SI). Pulsed emission was again coupled via the single-mode fiber and the RF configuration into cryostat 2 to resonantly excite

the selected QD. The corresponding photon autocorrelation function was recorded at an excitation power of 22 nW and is presented in Fig. 5a. Pulsed emission of light is clearly identified by the train of correlation pulses separated by 6.4 ns, and triggered single-photon emission is evidenced by the strongly reduced peak at zero delay with  $g^{(2)}(0) = 2\%$ . The zoom-in presentation  $g^{(2)}(\tau)$  in the inset of Fig. 5a shows a characteristic substructure of the central  $g^{(2)}(\tau)$  peak with a minimum at  $\tau = 0$  and side-peaks at finite delay. This correlation feature indicates that the non-ideal multi-photon suppression is mainly due to repeated QD excitation and decay within one single long-lasting laser pulse. Numerical modelling (red solid trace, cf. SI for details) was used to confirm the nature of the central correlation feature and to extract the lifetime of  $T_1 = 510$  ps and the pulse area of  $0.9\pi$  by fitting the modelled curve to the experimental data. Indeed, it was shown that both increased pulse length<sup>35</sup> and increased pulse area,<sup>36</sup> increase the probability of multiphoton-photon events. Thus, even better multi-photon suppression may be achieved by applying shorter electrical pulses to the microlaser in the future.

Finally, we study the photon-indistinguishability of emission under pulsed microlaser-excitation via a fiber-coupled Hong-Ou-Mandel two-photon interferometer with adjustable delay.<sup>26,37</sup> Here, the delay of the associated Mach-Zehnder interferometer was matched to the pulse repetition rate of 6.4 ns of the electrical voltage source used to drive the microlaser. The resulting photon-correlation diagram of emission from the resonantly excited QD is displayed in Fig. 5b both in co-polarized and cross-polarized measurement configuration. The experimental data is displayed as light blue and light gray lines, fitted numerically modelled data (see SI) is displayed as dark blue and dark gray lines. The only fitting parameter (except for background counts and scaling) is the imbalance of the second beam splitter, the one at which the HOM effect happens, turning out to be 8:9 and resulting in different height of the peaks at  $\pm 6.4$  ns. A significant degree of photon indistinguishability is evidenced by strongly reduced coincidences in the co-polarized case, while for the cross-polarized case we observe  $g_{\perp}^{(2)}(0) \approx 0.5$  as expected for distinguishable photons. In order to determine the resulting two-photon interference visibility  $V$ , we first integrate areas  $A_n^{\parallel,\perp}$  of the peaks centered at time delays  $\tau = n \times 6.4$  ns,  $n \in \{-7, -6, -5, \dots, 6, 7\}$  for each polarization configuration. Then, following

$$A_{\text{ref}}^{\parallel,\perp} = \frac{1}{12} \sum_{n=2}^7 A_n^{\parallel,\perp} + A_{-n}^{\parallel,\perp}$$

$$V = 1 - \frac{A_0^{\parallel} A_{\text{ref}}^{\perp}}{A_{\text{ref}}^{\parallel} A_0^{\perp}} \quad (1)$$

we extract a raw two-photon interference visibility of  $V = 0.44(4)$ . When compensating for the non-zero  $g^{(2)}(0)$  and for slight HOM beam-splitter imbalance of 8:9, we ob-



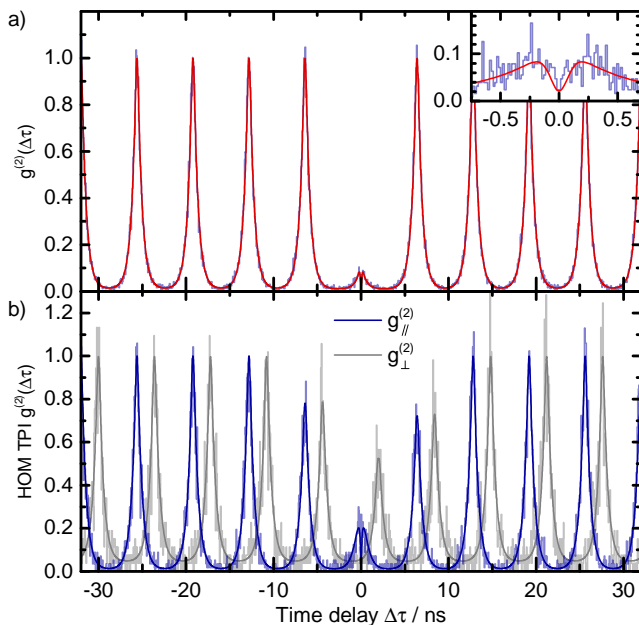


Figure 5. Demonstration of triggered single-photon emission and photon indistinguishability under pulsed microlaser excitation: **a)** Second-order photon auto-correlation under pulsed resonant excitation of the QD (pulse area:  $0.9\pi$ ). Triggered single-photon emission is clearly demonstrated by strong anti-bunching with  $g^{(2)}(0) \ll 0.5$ . The inset shows that the non-ideal  $g^{(2)}(0)$ -value can mainly be attributed to repeated QD excitation and decay within one single long-lasting laser pulse. This interpretation is confirmed by numeric modelling (red solid trace). **b)** HOM-histograms measured under copolarized and cross-polarized (shifted by  $\delta\tau = 2$  ns for the sake of clarity) configuration, respectively. Taking into account the non-ideal  $g^{(2)}(0)$ -value of the data presented in panel **a** we determine a HOM-visibility of  $V_{\text{pure}} = 0.57(9)$ .

tain a two-photon visibility as high as  $V_{\text{pure}} = 0.57(9)$  (see SI for details). This value is higher than 41% reported in Ref.<sup>22</sup> for direct non-resonant electrical excitation of a QD via carrier injection in a pin-diode design. It is, however, significantly lower than values exceeding 90% achieved by resonant-excitation via standard mode-locked lasers with ps-pulse widths. In order to explain the non-ideal degree of photon-indistinguishability one can consider several possible reasons such as temperature induced dephasing,<sup>26,38</sup> spectral fluctuations.<sup>26</sup> In the present case, i.e. under resonant excitation at low temperature, we can exclude these effects. Instead, we attribute the reduced HOM-visibility mainly to the rather long optical pulse width of 200 ps and to the non-Fourier-limited dephasing time  $T_2 = 0.5$  ns  $\approx T_1 < 2T_1$  (see Fig. S9). The increased laser pulse-width in combination with strong pulse-power ( $0.9\pi$ ) leads to two-photon fluorescence pulses and in turn results in reduced HOM-visibility.<sup>35,36,39</sup> On the other hand, non-Fourier-limited  $T_2$  directly makes photons more distinguishable: Be it due to random phase changes or be it due to finestruc-

ture splitting<sup>8,40</sup> of the QD transition and the thereby implied wavelength distinguishability. We therefore expect a strong improvement of the photon-indistinguishability by carefully adjusting the detected polarization to one single QD transition only and by reducing the optical pulse-length in future studies.

## METHODS

**Sample Technology** The QD-microlaser and the resonantly excited QD are based on AlGaAs heterostructures grown by molecular beam epitaxy. Both structures consist of high-quality AlAs/GaAs based on distributed Bragg-reflectors (DBRs) forming a planar microcavity with a central one- $\lambda$  GaAs cavity. A single layer of InGaAs quantum dots acts as active medium. In case of the microlaser, the planar microcavity is composed by a rather high number of 27 and 23 mirror pairs in the n-doped lower and p-doped upper DBR to ensure pronounced light-matter interaction and high- $\beta$  lasing. A dense array of micropillar lasers with a diameter of 3  $\mu\text{m}$  and a pitch of 60  $\mu\text{m}$  are realized by high-resolution electron-beam lithography and subsequent reactive-ion etching. The sample is planarized with benzocyclobutene (BCB) to mechanically support the ring-shaped upper Au-contacts, with the positive side-effect of protecting the AlAs layers from oxidizing. The realized array includes 62 electrically micropillar lasers emitting in the spectral range 912-919 nm. We refer to Ref.<sup>41</sup> for further details on the fabrication of electrically contacted micropillars. The QD sample used for the resonance fluorescence experiments has a more asymmetric microcavity design with 24 and 5 mirror pairs in the lower and upper DBR which fosters directional outcoupling of light with an extraction efficiency of up to 42%.<sup>42</sup> Due to the low QD density of  $2 \times 10^9$  cm<sup>-2</sup> and the presence of random photonic defects this planar microcavity sample is very suitable for single QD experiments without the need of lateral device processing.

**Experimental setup** The experimental configuration consists of two optical tables, each of which includes a Helium-flow cryostat (cryostat 1 and cryostat 2, respectively). The electrically driven QD-microlaser is installed in cryostat 1 and a single-mode fiber guides the laser light to the resonance fluorescence configuration in cross polarization configuration<sup>15,43,44</sup> at cryostat 2. The resonant laser light enters the RF setup via a fiber beamsplitter where it is superimposed with a low power non-resonant support laser. The latter is a red diode laser (emission wavelength: 670 nm) whose emission fills charge traps adjacent to the quantum dot to effectively gate RF signal of the QD.<sup>45</sup> The combined lasers are collimated again to free space and are aligned with the RF detection beam path by means of a polarizing beam splitter cube (PBS). Excitation of the quantum dot and detection of RF is then performed confocally through a  $NA = 0.65$ ,  $f = 4$  mm microscope objective. The main purpose of

the PBS is to strongly suppresses laser light reflected from the sample. In order to compensate for possible polarization ellipticity and to maximize laser stray-light suppression, a quarter-wave plate is placed in the excitation/detection path between PBS and microscope objective.<sup>44</sup> The detected light is fed into a polarization-maintaining single-mode fiber, both for spatial filtering and to facilitate quantum-optics experiments. For HBT- and HOM-style single-photon correlation experiments, superconducting single-photon detectors (SSPDs) with a time resolution FWHM of 55 ps are correlated. High resolution RF spectra are recorded by means of a scanning Fabry-Perot interferometer with 100 MHz spectral resolution.

## CONCLUSION

In summary we demonstrated a fully nanophotonic concept to control single-photon emission of a solid-state two-level system. The concept applies an electrically driven high- $\beta$  microlaser which resonantly drives a semiconductor QD acting as two-level system. It shows for the first time applicability of micro- and nano-laser in advanced quantum-optics experiments under strict resonant excitation. Temperature induced spectral fine-tuning of a suitable microlaser-QD allows us to observe dressing of the fundamental QD transition and the occurrence of Rabi-oscillations in photon-correlation measurements. Pulsed electrical excitation of the microlaser leads the emission of single photons with high multi-photon suppression ( $g^{(2)}(0) = 2\%$ ) and a Hong-Ou-Mandel vis-

ibility as high as 57%. As such our results present the great potential of combining and coupling nanophotonic devices to systems with enhanced functionality. In the future, our concept could be further developed into a fully integrated on-chip resonantly pumped quantum light sources with many interesting applications in photonic quantum information technology.

## ACKNOWLEDGEMENTS

The research leading to these results has received funding from from the European Research Council (ERC) under the European Union's Seventh Framework ERC Grant Agreement No. 615613, from the German Research Foundation via CRC 787 and Projects No. RE2974/5-1, RE2974/9-1 and SCHN1376/2-1, the State of Bavaria and the German Ministry of Education and Research (BMBF) within Q.com-H.

## AUTHOR CONTRIBUTIONS

S.R. initiated the research and conceived the experiments. S.K. and T.G. performed the experiments. X.P. and S.R. supervised the experiments. A.C. did the continuous wave theoretical analysis, S.K. did the pulsed theoretical analysis. M.S. built the resonance fluorescence setup. M.E., C.S. and S.H. realized the samples. S.R. and S.K. wrote the manuscript with contributions from all other authors.

---

\* Correspondence and requests for materials should be addressed to S.R., e-mail address: stephan.reitzenstein@physik.tu-berlin.de

<sup>1</sup> Gisin, N. & Thew, R. Quantum communication. *Nat. Photonics* **1**, 165–171 (2007).

<sup>2</sup> Bouwmeester, D., Ekert, A. K. & Zeilinger, A. *The physics of quantum information: Quantum cryptography, quantum teleportation, quantum computation* (Springer, Berlin, 2010).

<sup>3</sup> Nielsen, M. A. & Chuang, I. L. *Quantum Computation and Quantum Information* (Cambridge University Press, Cambridge, 2010).

<sup>4</sup> Ladd, T. D. *et al.* Quantum computers. *Nature* **464**, 45–53 (2010).

<sup>5</sup> Aharonovich, I., Englund, D. & Toth, M. Solid-state single-photon emitters. *Nat. Photonics* **10**, 631–641 (2016).

<sup>6</sup> Michler, P. *et al.* A quantum dot single-photon turnstile device. *Science* **290**, 2282–2285 (2000).

<sup>7</sup> Santori, C., Pelton, M., Solomon, G., Dale, Y. & Yamamoto, Y. Triggered single photons from a quantum dot. *Phys. Rev. Lett.* **86**, 1502–1505 (2001).

<sup>8</sup> Santori, C., Fattal, D., Vučković, J., Solomon, G. S. & Yamamoto, Y. Indistinguishable photons from a single-photon device. *Nature* **419**, 594–597 (2002).

<sup>9</sup> Ester, P. *et al.* p-Shell Rabi-flopping and single photon emission in an InGaAs/GaAs quantum dot. *Physica E* **40**, 2004–2006 (2008).

<sup>10</sup> Heindel, T. *et al.* Electrically driven quantum dot-micropillar single photon source with 34% overall efficiency. *Appl. Phys. Lett.* **96**, 10–13 (2010).

<sup>11</sup> Gschrey, M. *et al.* Highly indistinguishable photons from deterministic quantum-dot microlenses utilizing three-dimensional in situ electron-beam lithography. *Nat. Commun.* **6**, 7662 (2015).

<sup>12</sup> Muller, A. *et al.* Resonance fluorescence from a coherently driven semiconductor quantum dot in a cavity. *Phys. Rev. Lett.* **99**, 187402 (2007).

<sup>13</sup> Vamivakas, A. N., Zhao, Y., Lu, C.-Y. & Atatüre, M. Spin-resolved quantum-dot resonance fluorescence. *Nat. Phys.* **5**, 198–202 (2009).

<sup>14</sup> He, Y.-M. *et al.* On-demand semiconductor single-photon source with near-unity indistinguishability. *Nat. Nano.* **1–11** (2013).

<sup>15</sup> Kuhlmann, A. V. *et al.* A dark-field microscope for background-free detection of resonance fluorescence from single semiconductor quantum dots operating in a set-and-forget mode. *Rev. Sci. Instrum.* **84**, 073905 (2013).

- <sup>16</sup> Ates, S. *et al.* Post-selected indistinguishable photons from the resonance fluorescence of a single quantum dot in a microcavity. *Phys. Rev. Lett.* **103**, 167402 (2009).
- <sup>17</sup> Hopfmann, C. *et al.* Efficient stray-light suppression for resonance fluorescence in quantum dot micropillars using self-aligned metal apertures. *Semicond. Sci. Technol.* **31**, 095007 (2016).
- <sup>18</sup> Matthiesen, C., Vamivakas, A. N. & Atatüre, M. Subnatural linewidth single photons from a quantum dot. *Phys. Rev. Lett.* **108**, 093602 (2012).
- <sup>19</sup> Ates, S. *et al.* Non-resonant dot-cavity coupling and its potential for resonant single-quantum-dot spectroscopy. *Nat. Photonics* **3**, 724–728 (2009).
- <sup>20</sup> Briegel, H.-J., Dür, W., Cirac, J. I. & Zoller, P. Quantum Repeaters: The Role of Imperfect Local Operations in Quantum Communication. *Phys. Rev. Lett.* **81**, 5932–5935 (1998).
- <sup>21</sup> Sangouard, N. *et al.* Long-distance entanglement distribution with single-photon sources. *Phys. Rev. A* **76**, 253 (2007).
- <sup>22</sup> Schlehahn, A. *et al.* An electrically driven cavity-enhanced source of indistinguishable photons with 61% overall efficiency. *APL Photonics* **1**, 011301 (2016).
- <sup>23</sup> Munnely, P. *et al.* Electrically Tunable Single-Photon Source Triggered by a Monolithically Integrated Quantum Dot Microlaser. *ACS Photonics* **4**, 790–794 (2017).
- <sup>24</sup> Stock, E. *et al.* On-chip quantum optics with quantum dot microcavities. *Adv. Mater.* **25**, 707–710 (2013).
- <sup>25</sup> Lee, J. P. *et al.* Electrically driven and electrically tunable quantum light sources. *Appl. Phys. Lett.* **110**, 071102 (2017).
- <sup>26</sup> Thoma, A. *et al.* Exploring Dephasing of a Solid-State Quantum Emitter via Time- and Temperature-Dependent Hong-Ou-Mandel Experiments. *Phys. Rev. Lett.* **116**, 033601 (2016).
- <sup>27</sup> Leymann, H. A. M. *et al.* Intensity fluctuations in bimodal micropillar lasers enhanced by quantum-dot gain competition. *Phys. Rev. A* **87** (2013).
- <sup>28</sup> Redlich, C. *et al.* Mode-switching induced super-thermal bunching in quantum-dot microlasers. *New J. Phys.* **18**, 063011 (2016).
- <sup>29</sup> Strauf, S. Self-Tuned Quantum Dot Gain in Photonic Crystal Lasers. *Phys. Rev. Lett.* **96**, 127404 (2006).
- <sup>30</sup> Ulrich, S. M. *et al.* Photon statistics of semiconductor microcavity lasers. *Phys. Rev. Lett.* **98**, 043906 (2007).
- <sup>31</sup> Kreinberg, S. *et al.* Emission from quantum-dot high- $\beta$  microcavities: Transition from spontaneous emission to lasing and the effects of superradiant emitter coupling. *Light Sci. Appl.* **6**, e17030 (2017).
- <sup>32</sup> Bayer, M. *et al.* Fine structure of neutral and charged excitons in self-assembled In(Ga)As/(Al)GaAs quantum dots. *Phys. Rev. B* **65**, 3216 (2002).
- <sup>33</sup> Mollow, B. R. Power Spectrum of Light Scattered by Two-Level Systems. *Phys. Rev.* **188**, 1969–1975 (1969).
- <sup>34</sup> Davanço, M., Hellberg, C. S., Ates, S., Badolato, A. & Srinivasan, K. Multiple time scale blinking in InAs quantum dot single-photon sources. *Phys. Rev. B* **89** (2014).
- <sup>35</sup> Fischer, K. A., Müller, K., Lagoudakis, K. G. & Vučković, J. Dynamical modeling of pulsed two-photon interference. *New J. Phys.* **18**, 113053 (2016).
- <sup>36</sup> Fischer, K. A. *et al.* Signatures of two-photon pulses from a quantum two-level system. *Nat. Phys.* **13**, 649–654 (2017).
- <sup>37</sup> Bennett, A. J. *et al.* Indistinguishable photons from a diode. *Appl. Phys. Lett.* **92**, 193503 (2008).
- <sup>38</sup> Varoutsis, S. *et al.* Restoration of photon indistinguishability in the emission of a semiconductor quantum dot. *Phys. Rev. B* **72**, 681 (2005).
- <sup>39</sup> Dada, A. C. *et al.* Indistinguishable single photons with flexible electronic triggering. *Optica* **3**, 493 (2016).
- <sup>40</sup> Gazzano, O. *et al.* Bright solid-state sources of indistinguishable single photons. *Nat. Commun.* **4**, 1425 (2013).
- <sup>41</sup> Böckler, C. *et al.* Electrically driven high-Q quantum dot-micropillar cavities. *Appl. Phys. Lett.* **92**, 091107 (2008).
- <sup>42</sup> Maier, S. *et al.* Bright single photon source based on self-aligned quantum dot-cavity systems. *Opt. Express* **22**, 8136–8142 (2014).
- <sup>43</sup> Unsleber, S. *et al.* Deterministic generation of bright single resonance fluorescence photons from a Purcell-enhanced quantum dot-micropillar system. *Opt. Express* **23**, 32977–32985 (2015).
- <sup>44</sup> Strauß, M. *et al.* Photon-statistics excitation spectroscopy of a single two-level system. *Phys. Rev. B* **93** (2016).
- <sup>45</sup> Nguyen, H. S. *et al.* Optically gated resonant emission of single quantum dots. *Phys. Rev. Lett.* **108**, 057401 (2012).